Insect Biochemistry and Molecular Biology 107 (2019) 1–9

Contents lists available at ScienceDirect

Insect Biochemistry and Molecular Biology

journal homepage: www.elsevier.com/locate/ibmb

Complement-like proteins TEP1, TEP3 and TEP4 are positive regulators of periostial hemocyte aggregation in the mosquito *Anopheles gambiae*

Yan Yan, Julián F. Hillyer*

Department of Biological Sciences, Vanderbilt University, Nashville, TN, USA

ARTICLE INFO

Keywords:
Immune system
Circulatory system
Dorsal vessel
Heart
Ostia
Hemocyte
Phagocytosis
Melanization

ABSTRACT

The mosquito immune and circulatory systems are functionally integrated. During an infection, hemocytes aggregate around the ostia (valves) of the dorsal vessel – areas of the heart called the periostial regions – where they phagocytose live and melanized pathogens. Although periostial hemocyte aggregation is an immune response that occurs following infection with bacteria and malaria parasites, the molecular basis of this process remains poorly understood. Here, we show that the thioester-containing proteins, TEP1, TEP3 and TEP4 are positive regulators of periostial hemocyte aggregation in the African malaria mosquito, *Anopheles gambiae*. RNAi-based knockdown of *TEP1*, *TEP3* and *TEP4* resulted in fewer periostial hemocytes following *Escherichia coli* infection, without affecting the adjacent population of non-periostial, sessile hemocytes. Moreover, knockdown of *TEP1*, *TEP3* and *TEP4* expression resulted in reduced bacterial accumulation and melanin deposition at the periostial regions. Finally, this study confirmed the role that TEP1 plays in reducing infection intensity in the hemocoel. Overall, this research shows that the complement-like proteins, TEP1, TEP3 and TEP4, are positive regulators of the functional integration between the immune and circulatory systems of mosquitoes.

1. Introduction

Bacteria, fungi and malaria parasites invade the mosquito hemocoel (body cavity) where they face immune responses and circulatory currents (Bartholomay and Michel, 2018; Hillyer, 2016). Immune responses are primarily mediated by hemocytes (immune cells) that either circulate with the hemolymph (blood) – called circulating hemocytes – or remain attached to tissues – called sessile hemocytes (Hillyer and Strand, 2014). The circulation of hemolymph is maintained by the bidirectional (anterograde and retrograde) contraction of a dorsal vessel that extends the length of the body and is divided into two contiguous segments: a heart in the abdomen and an aorta in the thorax (Glenn et al., 2010; Sigle and Hillyer, 2018a). Hemolymph enters the heart though 6 pairs of abdominal ostia (valves) and 1 pair of thoraco-abdominal ostia, and exits back into the hemocoel via excurrent openings located at the anterior and posterior ends of the mosquito (Glenn et al., 2010; Sigle and Hillyer, 2018a). When pathogens enter the hemocoel, they circulate with the hemolymph and often become sequestered and killed in the areas surrounding the abdominal ostia – called the periostial regions – with this sequestration being due to phagocytosis by a group of sessile hemocytes called periostial hemocytes (Hillyer et al., 2007; King and Hillyer, 2012). During the course of an infection, additional hemocytes exit circulation and aggregate at the periostial regions, thus amplifying this pathogen elimination response.

Periostial hemocyte aggregation preferentially occurs around the ostia that receive the most hemolymph flow, and is induced by Gram (+) and Gram(–) bacteria, malaria parasites, and soluble microbial components (King and Hillyer, 2012; Sigle and Hillyer, 2016). Periostial hemocytes occupy less than 5% of the abdominal wall, yet sequester more than 40% of pathogens present on the cuticular integument (King and Hillyer, 2013; Sigle and Hillyer, 2018b). Periostial hemocytes also phagocytose melanized pathogens, and presumably secrete humoral immune factors (Sigle and Hillyer, 2016). Therefore, periostial hemocyte aggregation highlights the functional integration between the immune and circulatory systems of mosquitoes.

The genetic factors that regulate periostial hemocyte aggregation remain largely unknown. Our laboratory recently showed that two immune genes in the Nimrod gene family – *Eater* and *Draper* – influence periostial hemocyte aggregation (Sigle and Hillyer, 2018c). However, given the modest effects that *Eater* and *Draper* have on this process, we hypothesized that additional genes regulate periostial hemocyte aggregation. Thioester-containing proteins (TEPs) are complement-like opsonins that bind pathogens and promote phagocytosis by hemocytes (Levashina et al., 2001; Moita et al., 2005; Nazario-Toole and Wu, 2017). TEP1, TEP3 and TEP4 regulate the phagocytosis of Gram(+)

* Corresponding author. Department of Biological Sciences, Vanderbilt University, VU Station B 35-1634, Nashville, TN, 37235, USA.
E-mail address: julian.hillyer@vanderbilt.edu (J.F. Hillyer).

https://doi.org/10.1016/j.ibmb.2019.01.007
Received 12 December 2018; Received in revised form 16 January 2019; Accepted 18 January 2019
Available online 25 January 2019
0965-1748/

and/or Gram(–) bacteria, and both TEP1 and TEP3 bind malaria parasites and mediate their lysis and melanization (Blandin et al., 2004; Fraiture et al., 2009; Garver et al., 2012; Levashina et al., 2001; Moita et al., 2005; Povelones et al., 2011, 2009). The pleiotropic functions of TEPs led us to hypothesize that they are also involved in periostial hemocyte aggregation. Here, we show that *TEP1*, *TEP3* and *TEP4* are positive regulators of periostial hemocyte aggregation in the African malaria mosquito, *Anopheles gambiae*, and thus, are involved in the functional integration between the immune and circulatory systems.

2. Materials and methods

2.1. Mosquito colony

Anopheles gambiae, Giles sensu stricto (G3 strain; Diptera: Culicidae), were maintained at 27 °C and 75% relative humidity (R.H.) under a 12 h:12 h light:dark photoperiod, as previously described (Glenn et al., 2010). Larvae were reared in deionized water and fed a mixture of 2.8 parts koi food and 1-part baker's yeast. Adults were maintained in 2.4 L plastic buckets and fed 10% sucrose.

2.2. RNA extraction and cDNA synthesis

RNA was extracted and isolated from ~10 whole-body mosquitoes using TRIzol Reagent (Invitrogen, Carlsbad, CA, USA), and purified using the RNeasy Mini Kit (Qiagen, Valencia, CA, USA). The concentration of RNA was quantified using a BioPhotometer Plus spectrophotometer (Eppendorf AG, Hamburg, Germany), and the RNA was treated with RQ1 RNase-free DNase (Promega, Madison, WI, USA). Up to 5 μg of RNA was then used for cDNA synthesis by means of an Oligo $(dT)_{20}$ primer and the SuperScript III First-Strand Synthesis System for RT-PCR (Invitrogen).

2.3. Double-stranded RNA (dsRNA) synthesis

Three mosquito-specific dsRNAs were synthesized: ds*TEP1*, ds*TEP3* and ds*TEP4*. One non-mosquito dsRNA – used as a negative control – was synthesized: ds*BLA(Ap^R)* (beta-lactamase) (Estévez-Lao and Hillyer, 2014; Sigle and Hillyer, 2018c). To synthesize the TEP dsRNAs, *A. gambiae* cDNA was subjected to PCR using gene-specific primers with T7 promoter tags (Table S1 in Supplementary File 1). Each amplicon was separated by agarose gel electrophoresis, excised, and purified using Qiagen's QIAquick Gel Extraction kit (Qiagen, Valencia, CA, USA). To increase the amount of template for dsRNA synthesis, each amplicon was then used as template for a second PCR reaction using the same primers. The product was purified using the QIAquick PCR Purification Kit (Qiagen, Valencia, CA, USA), and the concentration was quantified spectrophotometrically. Up to 1 μg of the second PCR product was used as template for dsRNA synthesis using the MEGAscript T7 Kit (Applied Biosystems). The resultant dsRNA was precipitated with ethanol and re-suspended in phosphate-buffered saline (PBS). The concentration of dsRNA was quantified spectrophotometrically and the integrity of dsRNA was verified by agarose gel electrophoresis. The same procedure was followed for ds*BLA(Ap^R)* synthesis, except that the starting material was DNA extracted from *Escherichia coli* BL21(DE3) containing the pET-46 plasmid (EMD Chemicals, Gibbstown, NJ).

2.4. RNA interference (RNAi), mosquito treatments, and bacterial rearing

Two-day-old female mosquitoes were anesthetized briefly by placing them in a Petri dish held over ice, and then injected 300 ng of dsRNA at the thoracic anepisternal cleft using a Nanoject III Programmable Nanoliter Injector (Drummond Scientific Company, Broomall, PA, USA). Four days after dsRNA injection, mosquitoes were divided into two groups: (1) not infected (left unmanipulated and herein termed “naïve”), and (2) infected by injecting 69 nL of tetracycline resistant, GFP-expressing *E. coli* (modified DH5α; GFP-*E. coli*). An injury group (e.g., sham injection) was not assayed because injury does not induce periostial hemocyte aggregation (King and Hillyer, 2013, 2012; Sigle and Hillyer, 2016). For infections, GFP-*E. coli* were grown overnight in Luria-Bertani's rich nutrient medium (LB) in a 37 °C shaking incubator (New Brunswick Scientific, Edison, NJ, USA). The absorbance of *E. coli* cultures was measured spectrophotometrically and normalized to $OD_{600} = 2$ prior to injection, and absolute doses were determined after plating in LB. Across experimental trials, the infection dose averaged at 38,330 *E. coli* per mosquito.

2.5. RNAi knockdown efficiency

RNA was purified from mosquitoes that were either naïve, or had been infected with *E. coli* for 4 h or 24 h. cDNA was synthesized and used as template for real-time quantitative PCR (qPCR) using gene-specific primers (Table S1 in Supplementary File 1) and Power SYBR Green PCR Master Mix (Applied Biosystems, Foster City, CA) on an ABI 7300 Real-Time PCR System. Relative quantification of mRNA levels was conducted using the $2_T^{-\Delta\Delta C}$ method, using the housekeeping gene *RPS7* as the reference gene (Coggins et al., 2012; Livak and Schmittgen, 2001). Three biological replicates were conducted with two technical replicates each. The absence of genomic DNA in the cDNA preparations was confirmed by melting curve analysis at the end of each qPCR run.

2.6. In vivo hemocyte staining and mosquito dissections

Hemocytes were stained *in vivo* using Vybrant CM-DiI Cell-Labeling Solution (Invitrogen) as previously described (King and Hillyer, 2012). Briefly, live mosquitoes were anesthetized and injected with 0.4 μl of a solution consisting of 67 μM CM-DiI and 1.08 mM Hoechst 33342 (Invitrogen) in PBS. Mosquitoes were incubated at 27 °C and 75% R.H. for 20 min, and then fixed for 10 min by injecting 16% formaldehyde into the hemocoel. The abdomens were immersed in PBS containing 0.1% Triton X-100, bisected along a coronal plane, and the internal organs were removed. The dorsal abdomens – containing the heart and periostial hemocytes – were rinsed briefly in PBS and mounted between a glass slide and a coverslip using Aqua-Poly/Mount (Polysciences; Warrington, PA, USA).

2.7. Microscopy and image acquisition

Each dorsal abdomen was imaged under bright-field and fluorescence illumination on a Nikon 90i compound microscope connected to a Nikon Digital Sight DS-Qi1 monochrome digital camera and Nikon's Advanced Research NIS Elements software (Nikon, Tokyo, Japan). Z-stacks were acquired using a linear encoded Z-motor. For image presentation and pixel intensity measurements, all images within a stack were combined into a two-dimensional, focused image using the Extended Depth of Focus (EDF) function in NIS Elements.

2.8. Quantification of hemocytes

Hemocytes were counted manually by examining all images within a Z-stack. A cell was counted as a hemocyte if it measured 9–18 μm in diameter and was labeled with both CM-DiI and Hoechst 33342 (Sigle and Hillyer, 2016). A cell was counted as a periostial hemocyte if it was adjacent to an ostium, and a cell was counted as a non-periostial, sessile hemocyte if it was attached to the abdominal wall in an area that was outside of the periostial regions (King and Hillyer, 2013, 2012). Periostial hemocytes were counted within abdominal segments 2–7 whereas non-periostial, sessile hemocytes were only counted on the dorsal abdominal wall of segments 4 and 5. Hemocytes were not counted on the aorta, the excurrent openings or the thoraco-abdominal ostia because few hemocytes are present there, and infection does not induce the aggregation of hemocytes at those locations (Sigle and

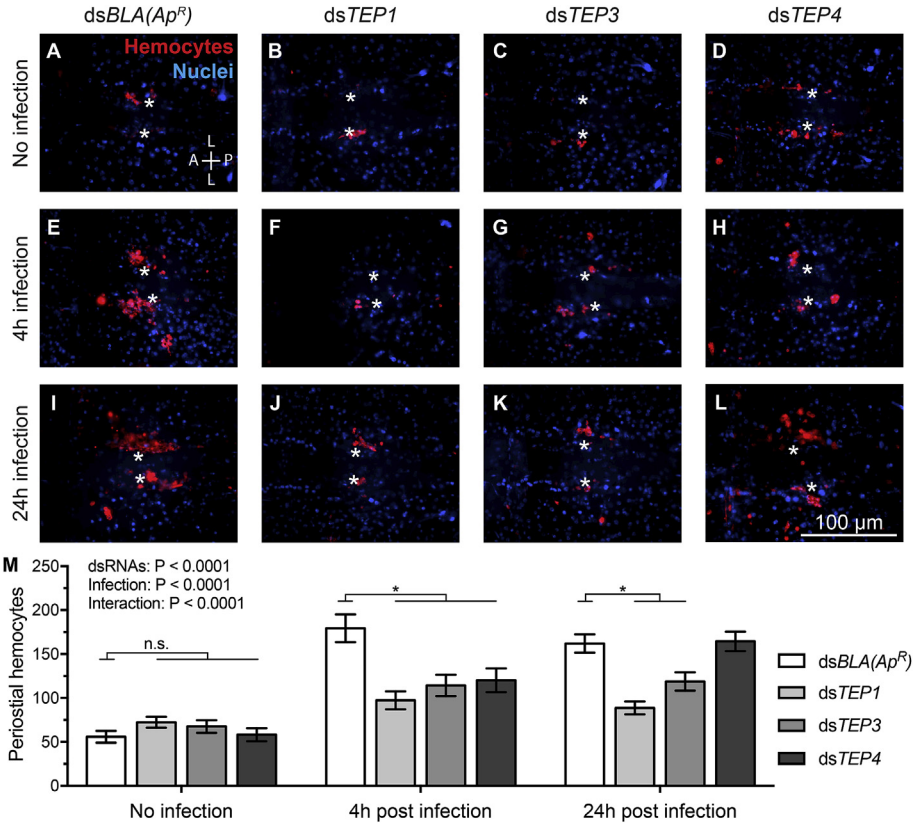

Fig. 1. *TEP1*, *TEP3* and *TEP4* knockdown mosquitoes have fewer periostial hemocytes following *E. coli* infection. (A–L) Fluorescence images of a single abdominal segment showing periostial hemocytes (stained red with CM-DiI) surrounding the ostia (asterisks) in naïve mosquitoes (A–D), and mosquitoes at 4 h (E–H) and 24 h (I–L) post-infection. Prior to infection, mosquitoes had been treated with ds*BLA(Ap^R)* (A, E, I), ds*TEP1* (B, F, J), ds*TEP3* (C, G, K) or ds*TEP4* (D, H, L). Nuclei were stained blue with Hoechst 33342. A, anterior; P, posterior; L, lateral. (M) Columns show the average number of periostial hemocytes in ds*BLA(Ap^R)*-, ds*TEP1*-, ds*TEP3*- and ds*TEP4*-injected mosquitoes that were not infected or had been infected with *E. coli* for 4 h or 24 h. Whiskers mark the standard error of the mean (S.E.M). Data were analyzed by two-way ANOVA, followed by Dunnett's post-hoc test. Asterisks indicate $P < 0.05$ (n.s., nonsignificant). (For interpretation of the references to colour in this figure legend, the reader is referred to the Web version of this article.)

Hillyer, 2018a, 2018b). Each treatment group contained a minimum of 16 mosquitoes that were assayed across 3 independent trials.

2.9. Quantification of GFP fluorescence at the periostial regions

GFP fluorescence intensity at the periostial regions was calculated from EDF images by measuring the sum pixel intensity above a threshold in NIS Elements (Sigle and Hillyer, 2018c, 2016). The threshold was defined as the pixel intensity that distinguished GFP emitted by *E. coli* rods (pixel intensity above the threshold) from background fluorescence intensity (pixel intensities below the threshold). Then, each periostial regions was delineated using the region of interest (ROI) tool, and the sum pixel intensity within each ROI was measured. Each treatment group contained a minimum of 15 mosquitoes that were assayed across 3 independent trials.

2.10. Quantification of dark deposits at the periostial regions

Dark deposits that result from melanization were quantified from EDF images by measuring the area of pixels with intensities below a threshold using NIS Elements (Sigle and Hillyer, 2016). For this, images were first examined to determine a pixel intensity that distinguished melanized areas (pixel intensities below the threshold) from non-melanized areas (pixel intensities above the threshold). Then, the area of pixels below the melanization threshold was measured for each periostial region ROI. A minimum of 19 mosquitoes across 3 independent trials were assayed for each treatment group.

2.11. Quantification of bacterial infection intensity

Infected mosquitoes were homogenized individually in PBS, and a dilution of each homogenate was spread on an LB agar plate containing tetracycline. Each plate was incubated at 37 °C overnight, and the resulting colony forming units (CFUs) were screened for GFP fluorescence on a Nikon SMZ1500 stereomicroscope and counted. The number of CFUs was used to calculate the number of live GFP-*E. coli* in each mosquito at the time of homogenization. Three independent trials were conducted with a minimum of 24 mosquitoes in each treatment group.

2.12. Statistical analyses

Data on RNAi knockdown efficiency, as well as hemocyte, pathogen or melanin aggregation, were analyzed by two-way ANOVA, followed by Dunn's multiple comparison test. The ds*BLA(Ap^R)*-injected mosquitoes were used as the reference group. The two-way ANOVA yields three distinct P values: (1) the dsRNA P value indicates whether knockdown of *BLA(Ap^R)*, *TEP1*, *TEP3* or *TEP4* affects the outcome, regardless of infection status; (2) the infection P value indicates whether the infection status affects the outcome, regardless of dsRNA treatment; (3) the interaction P value indicates whether the infection status has effects that depend on the dsRNA treatment. Data on bacterial infection intensity in the hemocoel were transformed by log 10 to satisfy the assumptions of ANOVA, and the transformed data were analyzed by two-way ANOVA as described above.

3. Results

3.1. TEP1, TEP3 and TEP4 are involved in infection-induced periostial hemocyte aggregation

To test whether TEPs are involved in periostial hemocyte aggregation, we knocked down the expression of *TEP1*, *TEP3* and *TEP4* by RNAi, which resulted in a > 71% reduction in mRNA levels relative to the control ds*BLA(Ap^R)*-injected mosquitoes (Fig. S1 in Supplementary File 1). Having established successful gene knockdown, we next quantified the number of periostial hemocytes in ds*TEP1*-, ds*TEP3*-, ds*TEP4*- and ds*BLA(Ap^R)*-injected mosquitoes that were naïve or had been infected with *E. coli* for 4 h or 24 h (Fig. 1). We found that the number of

periostial hemocytes in naïve mosquitoes remained unchanged regardless of gene knockdown. Furthermore, at 4 h and 24 h post *E. coli* infection, the ds*BLA(Ap^R)* mosquitoes had more periostial hemocytes than their naïve counterparts, again showing that periostial hemocyte aggregation is induced by infection. Knockdown of *TEP1*, *TEP3* and *TEP4* also resulted in an infection-induced increase in the number of periostial hemocytes, but this increase was significantly smaller than when mosquitoes were treated with ds*BLA(Ap^R)*. Specifically, at 4 h post-infection, the number of periostial hemocytes was 1.3-, 1.7-, and 2.1-fold higher in *TEP1*, *TEP3* and *TEP4* knockdown mosquitoes, relative to their respective naïve counterparts, which is significantly smaller than the 3.2-fold increase observed in ds*BLA(Ap^R)*-injected mosquitoes. This reduction in periostial hemocytes, relative to ds*BLA(Ap^R)*-injected mosquitoes, was maintained in *TEP1* and *TEP3* knockdown mosquitoes at 24 h post-infection. Therefore, these data show that knocking down the expression of *TEP1*, *TEP3* and *TEP4* does not affect the number of periostial hemocytes in naïve mosquitoes, but reduces the infection-induced aggregation of hemocytes at the periostial regions, with the phenotype being stronger in *TEP1*- and *TEP3*-depleted mosquitoes.

3.2. TEPs do not alter the spatial distribution of periostial hemocytes across segments

Periostial hemocytes preferentially aggregate around the ostia of abdominal segments 4, 5 and 6, which are the ostia that receive the majority of hemolymph flow (Sigle and Hillyer, 2016). Having established that TEPs facilitate the infection-induced aggregation of periostial hemocytes, we next sought to determine whether TEPs influence the spatial distribution of periostial hemocytes across the six periostial regions (Fig. 2). In naïve mosquitoes, the majority of periostial hemocytes were located in abdominal segments 4–7, and dsRNA treatments did not affect the segmental distribution of periostial hemocytes (interaction $P = 0.4062$). At 4 h post-infection, all segments had fewer periostial hemocytes in the *TEP1*, *TEP3* and *TEP4* knockdown mosquitoes than in ds*BLA(Ap^R)*-injected mosquitoes, but most periostial hemocytes remained in abdominal segments 4–6 and there was no difference in the spatial distribution of periostial hemocytes between the dsRNA groups. The same was true at 24 h post-infection, except that there was an interaction between the segmental distribution of periostial hemocytes and dsRNA treatment. Visual inspection of the data suggests that this change was due to *TEP4*-depleted mosquitoes displaying a non-proportional increase in periostial hemocytes within abdominal segments 4, 5 and 7. Altogether, these data show that knocking down the expression of *TEP1*, *TEP3* and *TEP4* does not have a meaningful effect on the spatial distribution of periostial hemocytes.

3.3. TEPs do not affect the number of sessile hemocytes outside the periostial regions

We next tested whether TEPs influence the aggregation of sessile hemocytes outside of the periostial regions, and did so to determine whether the effect of TEP depletion is limited to the periostial regions. To achieve this, we examined the same mosquitoes analyzed for Figs. 1 and 2 (the same Z-stacks), and quantified the number of non-periostial sessile hemocytes present on the dorsal portion of abdominal segments 4 and 5. We found that infection induces a modest increase in the number of non-periostial sessile hemocytes (Fig. 3; e.g., at 24 h post-infection there was a 0.4-fold increase in segment 4 for naïve ds*BLA(Ap^R)*-injected mosquitoes), but this increase is small relative to the increase in the number of periostial hemocytes (Fig. 2; e.g., at 24 h post-infection there was a 2.93-fold increase in segment 4 for naïve ds*BLA(Ap^R)*-injected mosquitoes). Furthermore, the number of non-periostial sessile hemocytes in *TEP1*, *TEP3* and *TEP4* knockdown mosquitoes was similar to those in ds*BLA(Ap^R)*-injected mosquitoes (Fig. 3). Therefore, knocking down the expression of *TEP1*, *TEP3* and *TEP4* does not affect sessile hemocytes located outside of the periostial regions.

3.4. TEPs do not play a major role in the accumulation of live bacteria at the periostial regions

Periostial hemocytes eliminate pathogens by phagocytosis, a cellular immune process that occurs within the periostial regions and elsewhere, and results in the capture and degradation of microbes (Hillyer and Strand, 2014; King and Hillyer, 2012). The hemocyte-based capture of GFP-*E. coli* at the periostial regions results in green fluorescence that accumulates as additional bacteria are phagocytosed, but dissipates as the bacteria are degraded (Sigle and Hillyer, 2016). Given that TEPs regulate periostial hemocyte aggregation, and that TEPs are regulators of the phagocytosis response (Blandin and Levashina, 2007; Moita et al., 2005), we next sought to assay whether knocking down the expression of *TEP1*, *TEP3* and *TEP4* affects *E. coli* accumulation at the periostial regions. To achieve this, we quantified the fluorescence intensity of GFP-*E. coli* at the periostial regions of dsTEP- and ds*BLA(Ap^R)*-injected mosquitoes at 4 h or 24 h post-infection. To our surprise, we did not detect significant differences in the fluorescence intensity of GFP-*E. coli* between the *TEP1*, *TEP3* and *TEP4* knockdown and the ds*BLA(Ap^R)*-injected mosquitoes at either 4 h or 24 h post-infection (Fig. 4). However, at 4 h there was a trend for all dsTEP groups to have less fluorescence at the periostial regions than the ds*BLA(Ap^R)* group, providing weak evidence of overall phagocytic reduction in mosquitoes where *TEP1*, *TEP3* and *TEP4* had been knocked down. Furthermore, between 4 h and 24 h post-infection the ds*BLA(Ap^R)*- and ds*TEP4*-injected mosquitoes experienced significant reductions ($p < 0.05$) in GFP fluorescence intensity at the periostial regions – 68% and 55% reductions, respectively – whereas ds*TEP1*- and ds*TEP3*-injected mosquitoes experienced smaller, nonsignificant reductions ($p > 0.05$) of 39% and 41%, respectively. Overall, these data suggest that TEPs are not major regulators of bacterial accumulation at the periostial regions, although knocking down *TEP1* or *TEP3* results in slower bacterial clearance at the periostial regions.

3.5. TEPs regulate melanin accumulation on the surface of the heart

Hemocytes produce and secrete the enzymes that drive the phenoloxidase-based enzymatic cascade that leads to the melanization of pathogens, and when visualized by bright-field microscopy, the products of melanization can be seen as dark deposits (Hillyer, 2016; League and Hillyer, 2016; Michel et al., 2005; Sigle and Hillyer, 2016; Yassine et al., 2014). At the periostial regions, these dark deposits appear because of the phagocytosis of melanized pathogens by periostial hemocytes (Sigle and Hillyer, 2016). Given that TEPs regulate hemocyte aggregation but do not appear to play a major role in the accumulation of live bacteria at the periostial regions, we tested whether TEPs influence the accumulation of melanin at the periostial regions by means of a microscopy-based optical density assay (Fig. 5). As expected, melanin was absent in the periostial regions of naïve mosquitoes, regardless of dsRNA treatment. Upon infection, melanin accumulated at the periostial regions and co-localized with hemocytes, indicating the melanin had been phagocytosed. In ds*BLA(Ap^R)*-injected mosquitoes, by 4 h post-infection the area of the periostial regions that contained melanin increased 19.22-fold relative to naïve mosquitoes, and by 24 h post-infection it increased 37.5-fold (Fig. 5). But in ds*TEP1*-, ds*TEP3*- and ds*TEP4*-injected mosquitoes, at 4 h post-infection the melanized area increased only slightly – 1.68-, 4.55- and 5.79-fold, respectively, and this modest increase was sustained at 24 h post-infection in ds*TEP1*- and ds*TEP3*-injected mosquitoes. Therefore, this shows that knocking down the expression of *TEP1*, *TEP3* and *TEP4* reduces melanin accumulation at the periostial regions, with the phenotype being stronger in *TEP1*- and *TEP3*-depleted mosquitoes. These data, together with the GFP-*E. coli* fluorescence intensity data, suggest that *TEP1* and *TEP3* regulate pathogen elimination at the periostial regions.

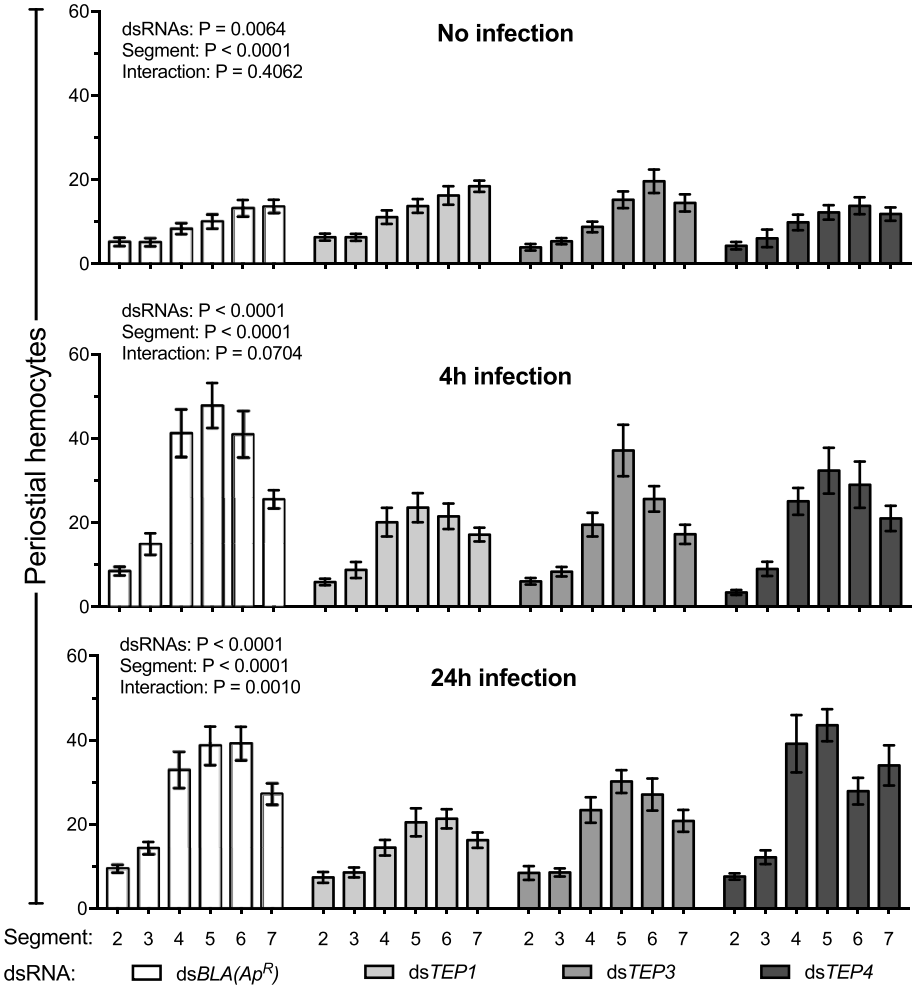

Fig. 2. TEPs do not meaningfully alter the spatial distribution of periostial hemocytes. Columns show the average number of periostial hemocytes at each periostial region in abdominal segments 2–7 in ds*BLA(Ap^R)*-, ds*TEP1*-, ds*TEP3*- and ds*TEP4*-injected mosquitoes that were not infected, or had been infected with *E. coli* for 4 h or 24 h. Whiskers mark the S.E.M. Data were analyzed by two-way ANOVA, followed by Dunnett's post-hoc test.

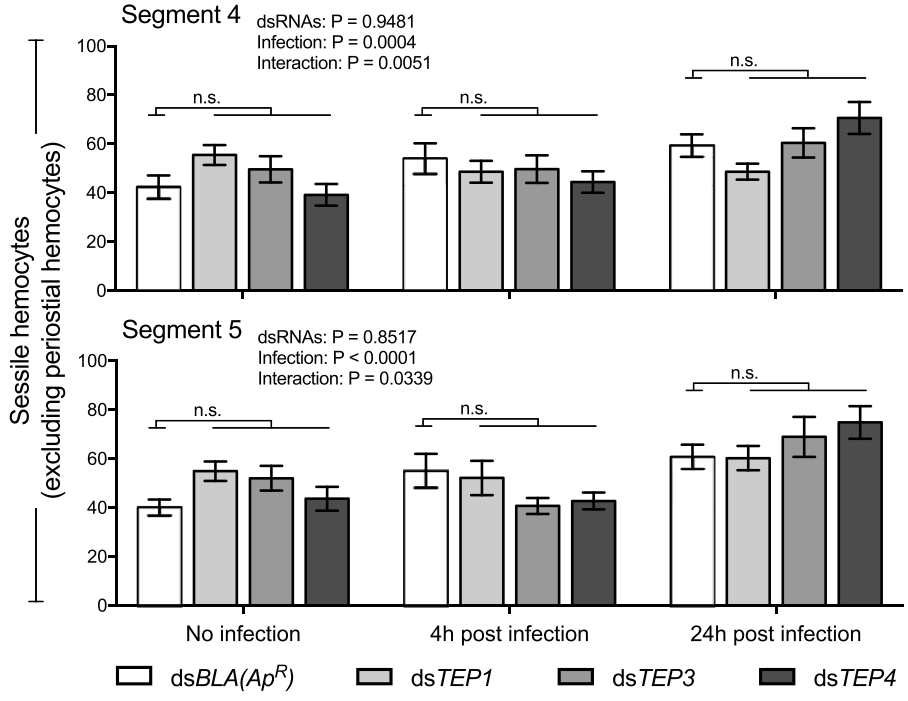

Fig. 3. TEPs do not affect the aggregation of sessile hemocytes outside the periostial regions. Columns show the average number of non-periostial sessile hemocytes on the dorsal abdomen of segments 4 (top) and 5 (bottom) in ds*BLA(Ap^R)*-, ds*TEP1*-, ds*TEP3*- and ds*TEP4*-injected mosquitoes that were not infected, or had been infected for 4 h or 24 h. Whiskers mark the S.E.M. Data were analyzed by two-way ANOVA, followed by Dunnett's post-hoc test (n.s., nonsignificant).

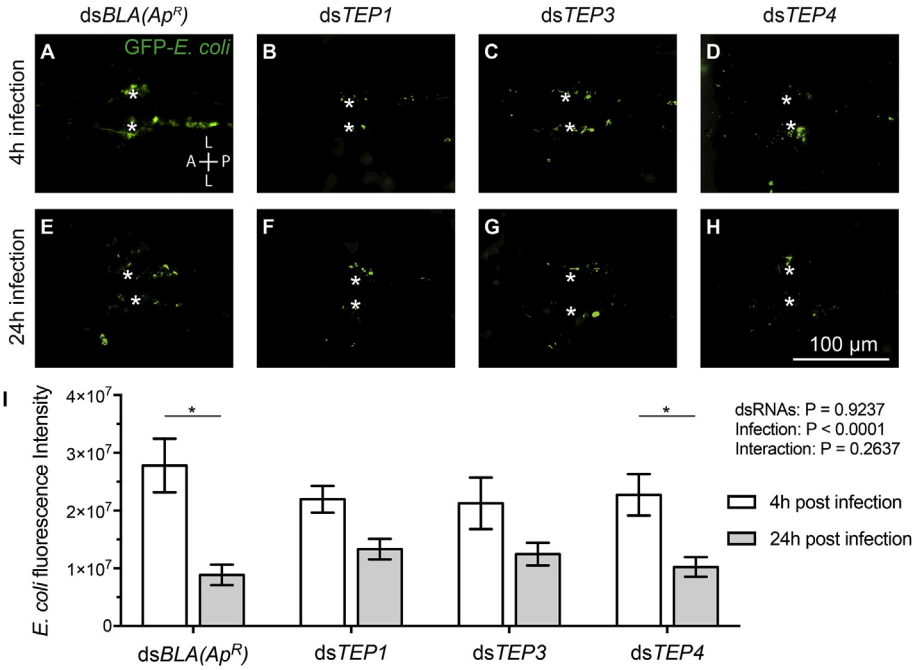

Fig. 4. TEPs do not play a major role in *E. coli* accumulation in the periostial regions. (A–H) Fluorescence images of a single abdominal segment showing GFP-*E. coli* around the ostia (asterisks) at 4 h (A–D) and 24 h (E–H) post-infection. Prior to infection, mosquitoes had been treated with ds*BLA(Ap^R)* (A, E), ds*TEP1* (B, F), ds*TEP3* (C, G) or ds*TEP4* (D, H). A: anterior; P: posterior; L: lateral. (I) Columns show the average GFP-*E. coli* fluorescence intensity in ds*BLA(Ap^R)*-, ds*TEP1*-, ds*TEP3*- and ds*TEP4*-injected mosquitoes that had been infected with *E. coli* for 4 h or 24 h. Whiskers mark the S.E.M. Data were analyzed by two-way ANOVA, followed by Dunnett's post-hoc test. Asterisks indicate $P < 0.05$.

3.6. TEP1 regulates the antibacterial immune response in the whole body

Having established that TEPs regulate periostial hemocyte aggregation as well as the accumulation of melanin at the periostial regions, we tested whether knocking down *TEP1*, *TEP3* and *TEP4* affects the overall antibacterial immune response. For this, we used a plating assay to measure the number of *E. coli* in the whole body of dsTEP- and ds*BLA(Ap^R)*-injected mosquitoes that had been infected for 4 h or 24 h. The bacterial intensities were similar between the dsRNA groups at 4 h post-infection, however, at 24 h post-infection the TEP1-depleted mosquitoes had 251% more bacteria in their hemocoel than the ds*BLA(Ap^R)*-injected mosquitoes (Fig. 6). These data show that *TEP1* depletion suppresses the systemic antibacterial response.

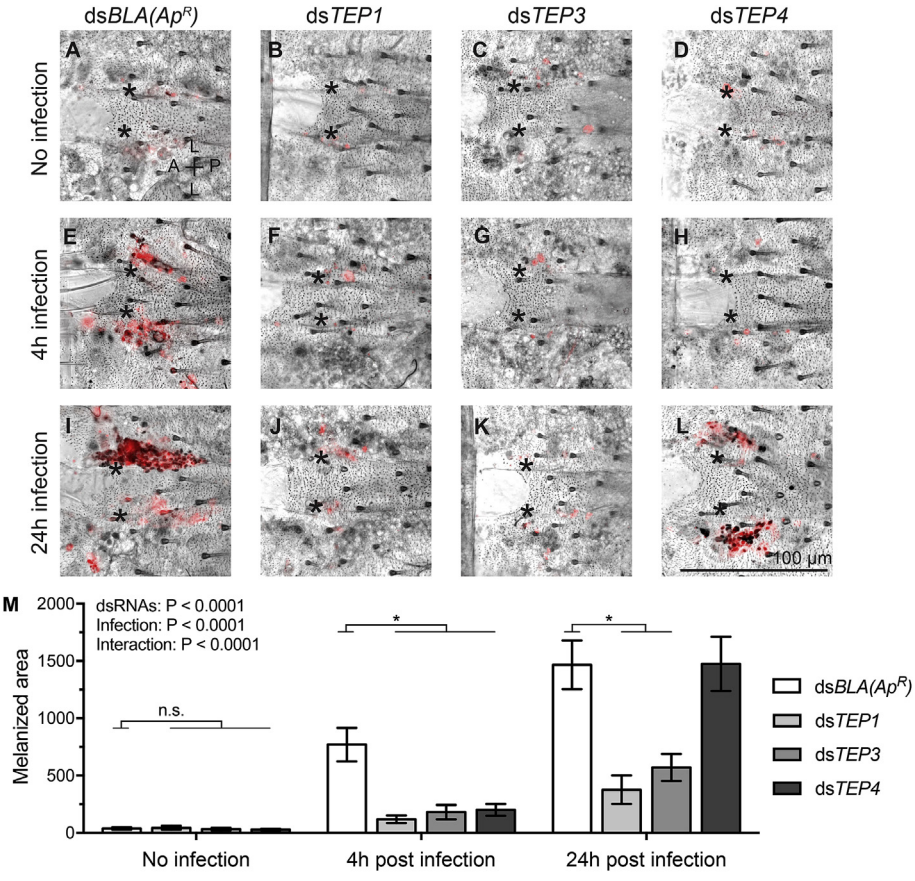

Fig. 5. TEPs regulate melanin accumulation at the periostial regions. (A–L) Bright field images of a single abdominal segment showing melanin deposits (black) captured by periostial hemocytes (red) surrounding the ostia (asterisks) in naïve mosquitoes (A–D), and mosquitoes at 4 h (E–H) and 24 h (I–L) post-infection. Prior to infection, mosquitoes had been treated with ds*BLA(Ap^R)* (A, E, I), ds*TEP1* (B, F, J), ds*TEP3* (C, G, K) or ds*TEP4* (D, H, L). A: anterior; P: posterior; L: lateral. (M) Columns show the average area with melanin deposits in ds*BLA(Ap^R)*-, ds*TEP1*-, ds*TEP3*- and ds*TEP4*-injected mosquitoes that were not infected or had been infected with *E. coli* for 4 h or 24 h. Whiskers mark the S.E.M. Data were analyzed by two-way ANOVA, followed by Dunnett's post-hoc test. Asterisks indicate $P < 0.05$ (n.s., nonsignificant). (For interpretation of the references to colour in this figure legend, the reader is referred to the Web version of this article.)

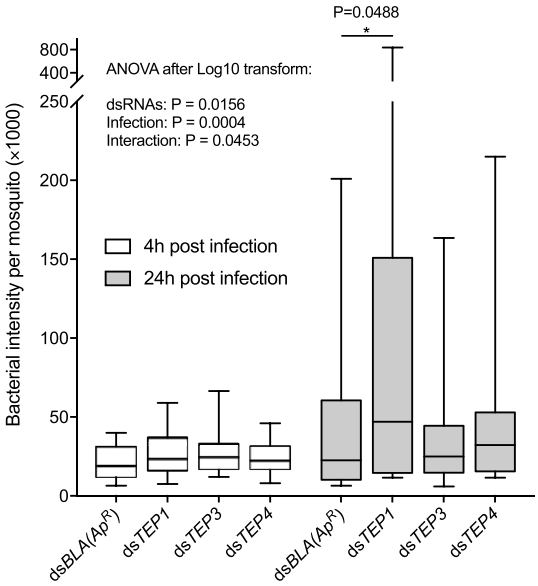

Fig. 6. *TEP1* regulates the antibacterial response in the mosquito hemocoel. In this box plot, the center line marks the median, the box shows 50% of the data, and the whiskers delineate the range of live, tetracycline-resistant, GFP-*E. coli* in the whole body of ds*BLA*(Ap^R)-, ds*TEP1*-, ds*TEP3*- and ds*TEP4*-injected mosquitoes at 4 h or 24 h post-infection. For statistical analyses, bacterial intensity was transformed by log 10 to conform to a normal distribution and then analyzed by two-way ANOVA, followed by Dunnett's post-hoc test. Asterisk indicated a significant difference at $P < 0.05$.

4. Discussion

The aggregation of hemocytes and pathogens on the heart of mosquitoes has been observed in larvae and adults – albeit differently in the two life stages – as well as in several other insects (Da Silva et al., 2012; Ghosh et al., 2015; Hernández-Martínez et al., 2017; League et al., 2017, 2015; League and Hillyer, 2016; Pereira et al., 2015; Stone et al., 2012). However, the genetic mechanisms that lead to the physiological interaction between the immune and circulatory systems remain poorly understood. In this study, we show that *TEP1*, *TEP3* and *TEP4* positively regulate periostial hemocyte aggregation, and also influence the accumulation of bacteria on the surface of the heart. Therefore, *TEP1*, *TEP3* and *TEP4* are positive regulators of the functional integration between the immune and circulatory systems.

TEPs serve important roles in the immunological function of hemocytes. For example, TEPs are secreted by hemocytes and fat body and bind to bacteria in the hemocoel and *Plasmodium* parasites in the midgut, leading to their killing (Blandin et al., 2004; Blandin and Levashina, 2007; Fraiture et al., 2009; Garver et al., 2012; Levashina et al., 2001; Moita et al., 2005; Povelones et al., 2011, 2009; Severo et al., 2018; Volohonsky et al., 2017). When TEPs bind bacteria, this promotes phagocytosis by hemocytes via two pathways: the *TEP1-TEP3-LRP1-CED6L* pathway and the *TEP4-BINT2-CED2L-CED5L* pathway (Moita et al., 2005). Two downstream molecules – LRP1 and BINT2 – are transmembrane proteins that have overlapping functions in phagocytosis and adhesion (Mantuano et al., 2010; Moita et al., 2006). In this study, we found evidence that *TEP1*, *TEP3* and *TEP4* regulate another hemocyte function: the infection-induced aggregation of hemocytes on the surface of the heart. We propose that when a TEP binds and opsonizes a pathogen, it activates signal transduction pathways that activate the phagocytic and adhesive properties of hemocytes, leading to their attachment to the periostial regions by adhesive capture. Throughout this study, we found that *TEP1* and *TEP3* have stronger effects on periostial responses than *TEP4*. The stronger phenotypes associated with *TEP1* and *TEP3* knockdown could be because (i) the TEP1/TEP3 signal transduction pathway has a stronger regulatory function in periostial hemocyte aggregation, (ii) TEP1 and TEP3 play a more prominent role in the response against *E. coli*, or (iii) TEP1 and TEP3 play a more prominent role in the general immune response. We hypothesize that the latter is most likely for two reasons. First, although TEP1, TEP3 and TEP4 each have significant effects on *Plasmodium* that depend on the specific mosquito-parasite combination, in *A. gambiae,* TEP1 and TEP3 eliminate more *Plasmodium berghei* oocysts than TEP4 (Mitri et al., 2015; Povelones et al., 2011). Second, LRP1 – which is downstream of TEP1 and TEP3 – plays a stronger role in phagocytosis by non-periostial, sessile hemocytes than BINT2 – which is downstream of TEP4 (Moita et al., 2005). The similar phenotypes following *TEP1* and *TEP3* knockdown might be due to both TEP1 and TEP3 participating in the same phagocytic pathway, which includes LRIM1, and presumably APL1C (Mitri et al., 2015; Moita et al., 2005; Povelones et al., 2011). Indeed, both the N- and C-termini of TEP1 and TEP3 interact with the LRIM1/APL1C complex, while only the N-terminal of TEP4 interact with this complex (Povelones et al., 2011).

We also found that although TEPs regulate periostial hemocyte aggregation, they do not play a major role in the aggregation of sessile hemocytes in non-periostial regions. Indeed, a previous report – as well the present study – showed that an infection induces minimal hemocyte aggregation at non-periostial regions, relative to the intense aggregation seen on the surface of the heart (King and Hillyer, 2013). We propose that the specific effect observed on the heart is in large part because of circulatory currents, especially given that the periostial regions experience 20 times more hemolymph flow than the rest of the abdomen (Andereck et al., 2010; Glenn et al., 2010). Therefore, circulating hemocytes flow through the periostial regions more frequently than through any other region of the abdomen, and we hypothesize that once activated by TEPs, hemocytes have a higher chance of attaching to the periostial regions than elsewhere. This hypothesis is further supported by the observation that more periostial hemocytes aggregate in the middle abdominal segments, which are the regions of the heart that receive the most hemolymph flow (Sigle and Hillyer, 2016). Examination of images published by others also show a similar spatial distribution of hemocytes, pathogens or melanin in mosquitoes (Hernández-Martínez et al., 2017; Lombardo et al., 2013; Michel et al., 2005; Sigle and Hillyer, 2016; Yassine et al., 2014). However, flow alone does not explain the specific aggregation of hemocytes on the surface of the heart because knockdown of *TEP1*, *TEP3* and *TEP4* does not affect non-periostial areas. Thus, other forces or factors must also be involved.

Circulating, sessile and periostial hemocytes phagocytose both unmelanized and melanized pathogens (Hillyer et al., 2003a, 2003b; King and Hillyer, 2012; Sigle and Hillyer, 2016). TEP1, TEP3 and TEP4 are known to regulate the phagocytic activity of sessile hemocytes that reside on the lateral abdominal wall. Specifically, all three genes regulate the phagocytosis of dead *E. coli* and TEP1 and TEP4 also regulate the phagocytosis of dead *Staphylococcus aureus* (Moita et al., 2005). Consistent with the previous study, we found weak evidence that depleting TEP1, TEP3 and TEP4 slightly impairs the accumulation of live *E. coli* at the periostial regions at 4 h post-infection, and although the precise kinetics of bacterial clearance following phagocytosis are not known, we propose that this is due to an overall reduction in phagocytic activity within the periostial regions. The magnitude in the reduction of pathogen accumulation was smaller than what was observed in Moita et al. (2005), but this may be because of the location of the body that was assayed or the differences in the methods used. First, we used live *E. coli* instead of dead *E. coli* particles and quantified pathogen accumulation at 4 h instead of 30 min post-challenge – meaning that bacterial replication was occurring in our study. Second, Moita et al. (2005) quenched the fluorescence of non-phagocytosed FITC bioparticles – which is something we were unable to do for GFP-expressing live *E. coli* – and so, in our study the bacteria present on the surface of hemocytes yielded a signal even without being phagocytosed. In

addition to the differences in methodology, there is an alternate explanation that we believe is even more likely. We have reported that melanin masks the fluorescence emitted by GFP-*E. coli* (League and Hillyer, 2016). Therefore, we hypothesize that, because mosquitoes treated with ds*BLA(Ap^R)* have more melanin in the periostial regions than mosquitoes treated with ds*TEP1*, ds*TEP3* and ds*TEP4*, the fluorescence values measured for ds*BLA(Ap^R)* mosquitoes underestimate the amount of bacteria in the periostial regions, meaning that the real difference between ds*BLA(Ap^R)* and ds*TEP1*, ds*TEP3* and ds*TEP4* knockdown mosquitoes is larger than measured. Regardless, our finding that depleting *TEP1*, *TEP3* and *TEP4* reduces melanin accumulation in the periostial regions, together with evidence that (i) melanized or partially melanized bacteria are phagocytosed by hemocytes and (ii) uncontrolled TEP1 activation results in melanin accumulation on the heart even in the absence of infection, supports the role of TEPs in influencing phagocytosis at the periostial regions (Hillyer et al., 2003a, 2003b; Sigle and Hillyer, 2016; Yassine et al., 2014).

Periostial hemocyte aggregation is a general immune response that is elicited by multiple types of infection (King and Hillyer, 2012; Sigle and Hillyer, 2016), and therefore, we hypothesize that multiple immune pathways drive this process. Previously, our lab showed that two members of the Nimrod gene family – *Eater* and *Draper* – are regulators of periostial hemocyte aggregation (Sigle and Hillyer, 2018c). Knocking down *Eater*, *TEP1* and *TEP3* results in a similar phenotype – fewer periostial hemocytes – whereas knocking down *Draper* results in a marginal increase in the number of periostial hemocytes. Regardless, the phenotypes observed following *TEP1*, *TEP3* and *TEP4* knockdown were generally stronger than the phenotypes observed following the knockdown of *Eater* or *Draper*. TEPs are secreted proteins while Eater and Draper are transmembrane proteins, and thus, it is likely that TEPs, Eater and Draper occupy distinct functions in the pathways that regulate periostial hemocyte aggregation.

To successfully transmit malaria to a vertebrate host, *Plasmodium* parasites must complete an obligatory migration inside the mosquito. As part of this migration, sporozoites released from oocysts on the midgut circulate with the hemolymph as they seek to invade the salivary glands (Hillyer et al., 2007; Severo and Levashina, 2014; Smith et al., 2014; Wang and Jacobs-Lorena, 2013). While sporozoites circulate with the hemolymph, only 19% invade salivary glands (Hillyer et al., 2007). The specific mechanisms for sporozoite killing in the hemocoel remain largely unknown, but some are captured and killed by the periostial hemocytes, which highlights the advantage of having hemocytes reside in areas of high hemolymph flow (Hillyer et al., 2007; King and Hillyer, 2012). TEP1, TEP3 and TEP4 mediate the killing of *Plasmodium* in the midgut (Blandin et al., 2004; Fraiture et al., 2009; Mitri et al., 2015; Povelones et al., 2011, 2009). We hypothesize that TEP1, TEP3 and TEP4 have additional roles in reducing the number of malaria parasites in mosquitoes, and propose that future studies investigate whether TEPs are involved in the periostial hemocyte-mediated killing of sporozoites circulating with the hemolymph.

Acknowledgements

We thank Ms. Tania Estévez-Lao and Dr. Scott Williams for helpful discussions and feedback on the manuscript. This work was supported by the U.S. National Science Foundation (NSF) grant IOS-1456844 to JFH. The funders had no role in study design, data collection and analysis, decision to publish, or preparation of the manuscript.

Appendix A. Supplementary data

Supplementary data to this article can be found online at https://doi.org/10.1016/j.ibmb.2019.01.007.

References

Andereck, J.W., King, J.G., Hillyer, J.F., 2010. Contraction of the ventral abdomen potentiates extracardiac retrograde hemolymph propulsion in the mosquito hemocoel. PLoS One 5 (9), e12943. https://doi.org/10.1371/journal.pone.0012943.

Bartholomay, L.C., Michel, K., 2018. Mosquito Immunobiology: The Intersection of Vector Health and Vector Competence. Annu. Rev. Entomol. 63, 145–167. https://doi.org/10.1146/annurev-ento-010715-023530.

Blandin, S., Shiao, S.-H., Moita, L.F., Janse, C.J., Waters, A.P., Kafatos, F.C., Levashina, E.A., 2004. Complement-like protein TEP1 is a determinant of vectorial capacity in the malaria vector *Anopheles gambiae*. Cell 116, 661–670. https://doi.org/10.1016/S0092-8674(04)00173-4.

Blandin, S.A., Levashina, E.A., 2007. Phagocytosis in mosquito immune responses. Immunol. Rev. 219, 8–16. https://doi.org/10.1111/j.1600-065X.2007.00553.x.

Coggins, S.A., Estevez-Lao, T.Y., Hillyer, J.F., 2012. Increased survivorship following bacterial infection by the mosquito *Aedes aegypti* as compared to *Anopheles gambiae* correlates with increased transcriptional induction of antimicrobial peptides. Dev. Comp. Immunol. 37, 390–401. https://doi.org/10.1016/j.dci.2012.01.005.

Da Silva, R., Da Silva, S.R., Lange, A.B., 2012. The regulation of cardiac activity by nitric oxide (NO) in the Vietnamese stick insect, *Baculum extradentatum*. Cell. Signal. 24, 1344–1350. https://doi.org/10.1016/j.cellsig.2012.01.010.

Estévez-Lao, T.Y., Hillyer, J.F., 2014. Involvement of the *Anopheles gambiae* Nimrod gene family in mosquito immune responses. Insect Biochem. Mol. Biol. 44, 12–22. https://doi.org/10.1016/j.ibmb.2013.10.008.

Fraiture, M., Baxter, R.H.G., Steinert, S., Chelliah, Y., Frolet, C., Quispe-Tintaya, W., Hoffmann, J.A., Blandin, S.A., Levashina, E.A., 2009. Two mosquito LRR proteins function as complement control factors in the TEP1-mediated killing of *Plasmodium*. Cell Host Microbe 5, 273–284. https://doi.org/10.1016/j.chom.2009.01.005.

Garver, L.S., Bahia, A.C., Das, S., Souza-Neto, J.A., Shiao, J., Dong, Y., Dimopoulos, G., 2012. *Anopheles* Imd pathway factors and effectors in infection intensity-dependent anti-*Plasmodium* action. PLoS Pathog. 8 (6), e1002737. https://doi.org/10.1371/journal.ppat.1002737.

Ghosh, S., Singh, A., Mandal, S., Mandal, L., 2015. Active hematopoietic hubs in *Drosophila* adults generate hemocytes and contribute to immune response. Dev. Cell 33, 478–488. https://doi.org/10.1016/j.devcel.2015.03.014.

Glenn, J.D., King, J.G., Hillyer, J.F., 2010. Structural mechanics of the mosquito heart and its function in bidirectional hemolymph transport. J. Exp. Biol. 213, 541–550. https://doi.org/10.1242/jeb.035014.

Hernández-Martínez, S., Sánchez-Zavaleta, M., Brito, K., Herrera-Ortiz, A., Ons, S., Noriega, F.G., 2017. Allatotropin: A pleiotropic neuropeptide that elicits mosquito immune responses. PLoS One 12 (4), e0175759. https://doi.org/10.1371/journal.pone.0175759.

Hillyer, J.F., 2016. Insect immunology and hematopoiesis. Dev. Comp. Immunol. 58, 102–118. https://doi.org/10.1016/j.dci.2015.12.006.

Hillyer, J.F., Barreau, C., Vernicks, K.D., 2007. Efficiency of salivary gland invasion by malaria sporozoites is controlled by rapid sporozoite destruction in the mosquito haemocoel. Int. J. Parasitol. 37, 673–681. https://doi.org/10.1016/j.ijpara.2006.12.007.

Hillyer, J.F., Schmidt, S.L., Christensen, B.M., 2003a. Rapid phagocytosis and melanization of bacteria and *Plasmodium* sporozoites by hemocytes of the mosquito *Aedes aegypti*. J. Parasitol. 89 (1), 62–69. https://doi.org/10.1645/0022-3395(2003)089[0062:rpamob]2.0.co;2.

Hillyer, J.F., Schmidt, S.L., Christensen, B.M., 2003b. Hemocyte-mediated phagocytosis and melanization in the mosquito *Armigeres subalbatus* following immune challenge by bacteria. Cell Tissue Res. 313, 117–127. https://doi.org/10.1007/s00441-003-0744-y.

Hillyer, J.F., Strand, M.R., 2014. Mosquito hemocyte-mediated immune responses. Curr. Opin. Insect Sci. 3, 14–21. https://doi.org/10.1016/j.cois.2014.07.002.

King, J.G., Hillyer, J.F., 2013. Spatial and temporal in vivo analysis of circulating and sessile immune cells in mosquitoes: hemocyte mitosis following infection. BMC Biol. 11, 55. https://doi.org/10.1186/1741-7007-11-55.

King, J.G., Hillyer, J.F., 2012. Infection-induced interaction between the mosquito circulatory and immune systems. PLoS Pathog. 8 (11), e1003058. https://doi.org/10.1371/journal.ppat.1003058.

League, G.P., Estévez-Lao, T.Y., Yan, Y., Garcia-Lopez, V.A., Hillyer, J.F., 2017. *Anopheles gambiae* larvae mount stronger immune responses against bacterial infection than adults: evidence of adaptive decoupling in mosquitoes. Parasites Vectors 10, 367. https://doi.org/10.1186/s13071-017-2302-6.

League, G.P., Hillyer, J.F., 2016. Functional integration of the circulatory, immune, and respiratory systems in mosquito larvae: pathogen killing in the hemocyte-rich tracheal tufts. BMC Biol. 14, 78. https://doi.org/10.1186/s12915-016-0305-y.

League, G.P., Onuh, O.C., Hillyer, J.F., 2015. Comparative structural and functional analysis of the larval and adult dorsal vessel and its role in hemolymph circulation in the mosquito *Anopheles gambiae*. J. Exp. Biol. 218, 370–380. https://doi.org/10.1242/jeb.114942.

Levashina, E.A., Moita, L.F., Blandin, S.A., Vriend, G., Lagueux, M., Kafatos, F.C., 2001. Conserved role of a complement-like protein in phagocytosis revealed by dsRNA knockout in cultured cells of the mosquito, *Anopheles gambiae*. Cell 104, 709–718. https://doi.org/10.1016/S0092-8674(01)00267-7.

Livak, K.J., Schmittgen, T.D., 2001. Analysis of relative gene expression data using real-time quantitative PCR and the $2^{-\Delta\Delta C}_{T}$ Method. Methods 25, 402–408. https://doi.org/10.1006/meth.2001.1262.

Lombardo, F., Ghani, Y., Kafatos, F.C., Christophides, G.K., 2013. Comprehensive genetic dissection of the hemocyte immune response in the malaria mosquito *Anopheles gambiae*. PLoS Pathog. 9 (1), e1003145. https://doi.org/10.1371/journal.ppat.

1003145.
Mantuano, E., Jo, M., Gonias, S.L., Campana, W.M., 2010. Low density Lipoprotein Receptor-related Protein (LRP1) regulates Rac1 and RhoA reciprocally to control Schwann cell adhesion and migration. J. Biol. Chem. 285, 14259–14266. https://doi.org/10.1074/jbc.M109.085126.
Michel, K., Budd, A., Pinto, S., Gibson, T.J., Kafatos, F.C., 2005. *Anopheles gambiae* SRPN2 facilitates midgut invasion by the malaria parasite *Plasmodium berghei*. EMBO Rep. 6, 891–897. https://doi.org/10.1038/sj.embor.7400478.
Mitri, C., Bischoff, E., Takashima, E., Williams, M., Eiglmeier, K., Pain, A., Guelbeogo, W.M., Gneme, A., Brito-Fravallo, E., Holm, I., Lavazec, C., Sagnon, N., Baxter, R.H., Riehle, M.M., Vernick, K.D., 2015. An evolution-based screen for genetic differentiation between *Anopheles* sister taxa enriches for detection of functional immune factors. PLoS Pathog. 11 (12), e1005306. https://doi.org/10.1371/journal.ppat.1005306.
Moita, L.F., Vriend, G., Mahairaki, V., Louis, C., Kafatos, F.C., 2006. Integrins of *Anopheles gambiae* and a putative role of a new β integrin, BINT2, in phagocytosis of *E. coli*. Insect Biochem. Mol. Biol. 36, 282–290. https://doi.org/10.1016/j.ibmb.2006.01.004.
Moita, L.F., Wang-Sattler, R., Michel, K., Zimmermann, T., Blandin, S., Levashina, E.A., Kafatos, F.C., 2005. In vivo identification of novel regulators and conserved pathways of phagocytosis in *A. gambiae*. Immunity 23, 65–73. https://doi.org/10.1016/j.immuni.2005.05.006.
Nazario-Toole, A.E., Wu, L.P., 2017. Phagocytosis in Insect Immunity. Adv. Insect Physiol. 52, 35–82. https://doi.org/10.1016/bs.aiip.2016.12.001.
Pereira, M.F., Rossi, C.C., de Queiroz, M.V., Martins, G.F., Isaac, C., Bossé, J.T., Li, Y., Wren, B.W., Terra, V.S., Cuccui, J., Langford, P.R., Bazzolli, D.M.S., 2015. *Galleria mellonella* is an effective model to study *Actinobacillus pleuropneumoniae* infection. Microbiology 161, 387–400. https://doi.org/10.1099/mic.0.083923-0.
Povelones, M., Upton, L.M., Sala, K.A., Christophides, G.K., 2011. Structure-function analysis of the *Anopheles gambiae* LRIM1/APL1C complex and its interaction with complement C3-like protein TEP1. PLoS Pathog. 7 (4), e1002023. https://doi.org/10.1371/journal.ppat.1002023.
Povelones, M., Waterhouse, R.M., Kafatos, F.C., Christophides, G.K., 2009. Leucine-rich repeat protein complex activates mosquito complement in defense against *Plasmodium* parasites. Science 324 (5924), 258–261. https://doi.org/10.1126/science.1171400.
Severo, M.S., Landry, J.J.M., Lindquist, R.L., Goosmann, C., Brinkmann, V., Collier, P., Hauser, A.E., Benes, V., Henriksson, J., Teichmann, S.A., Levashina, E.A., 2018. Unbiased classification of mosquito blood cells by single-cell genomics and high-content imaging. Proc. Natl. Acad. Sci. 115, E7568–E7577. https://doi.org/10.1073/pnas.1803062115.
Severo, M.S., Levashina, E.A., 2014. Mosquito defenses against *Plasmodium* parasites. Curr. Opin. Insect Sci. 3, 30–36. https://doi.org/10.1016/j.cois.2014.07.007.
Sigle, L.T., Hillyer, J.F., 2018a. Structural and functional characterization of the contractile aorta and associated hemocytes of the mosquito *Anopheles gambiae*. J. Exp. Biol. 221, jeb181107. https://doi.org/10.1242/jeb.181107.
Sigle, L.T., Hillyer, J.F., 2018b. Mosquito hemocytes associate with circulatory structures that support intracardiac retrograde hemolymph flow. Front. Physiol. 9, 1187. https://doi.org/10.3389/fphys.2018.01187.
Sigle, L.T., Hillyer, J.F., 2018c. *Eater* and *draper* are involved in the periostial haemocyte immune response in the mosquito *Anopheles gambiae*. Insect Mol. Biol. 27, 429–438. https://doi.org/10.1111/imb.12383.
Sigle, L.T., Hillyer, J.F., 2016. Mosquito hemocytes preferentially aggregate and phagocytose pathogens in the periostial regions of the heart that experience the most hemolymph flow. Dev. Comp. Immunol. 55, 90–101. https://doi.org/10.1016/j.dci.2015.10.018.
Smith, R.C., Vega-Rodríguez, J., Jacobs-Lorena, M., 2014. The *Plasmodium* bottleneck: malaria parasite losses in the mosquito vector. Mem. Inst. Oswaldo Cruz 109, 644–661. https://doi.org/10.1590/0074-0276130597.
Stone, E.F., Fulton, B.O., Ayres, J.S., Pham, L.N., Ziauddin, J., Shirasu-Hiza, M.M., 2012. The circadian clock protein timeless regulates phagocytosis of bacteria in *Drosophila*. PLoS Pathog. 8 (1), e1002445. https://doi.org/10.1371/journal.ppat.1002445.
Volohonsky, G., Hopp, A.K., Saenger, M., Soichot, J., Scholze, H., Boch, J., Blandin, S.A., Marois, E., 2017. Transgenic expression of the anti-parasitic factor TEP1 in the malaria mosquito *Anopheles gambiae*. PLoS Pathog. 13 (1), e1006113. https://doi.org/10.1371/journal.ppat.1006113.
Wang, S., Jacobs-Lorena, M., 2013. Genetic approaches to interfere with malaria transmission by vector mosquitoes. Trends Biotechnol. 31, 185–193. https://doi.org/10.1016/j.tibtech.2013.01.001.
Yassine, H., Kamareddine, L., Chamat, S., Christophides, G.K., Osta, M.A., 2014. A serine protease homolog negatively regulates TEP1 consumption in systemic infections of the malaria vector *Anopheles gambiae*. J. Innate Immun. 6, 806–818. https://doi.org/10.1159/000363296.